JOTCS B
Journal of the Turkish Chemical Society
Section: B
Chemical Engineering
TURKISH CHEMICAL SOCIETY

Investigating the Chemical and Thermal Based Treatment Procedures on the Clinoptilolite to Improve the Physicochemical Properties

Ezgi Bayrakdar Ates[1*]

[1]Yalova University, Energy Systems Engineering Department, Yalova, 77100, Turkey.

Abstract: Natural clinoptilolites have been preferred as promising catalysts and adsorption materials due to their low cost and important properties. However, they struggle with their cationic phases and impurities, weakening the physicochemical structure. The main approach is to improve the features of clinoptilolites by applying treatments such as acid modification and calcination. Here in clinoptilolites in two different particle sizes were pre-treated with acid, then, calcined at two different temperatures (300 and 500 °C) with different durations (2 and 3 h). The effects of pre-treatment were investigated with X-ray diffraction (XRD), X-ray fluorescence (XRF), Fourier transform infrared (FTIR), Thermogravimetry (TG-DTG), Differential Thermal Analysis (DTA), N_2 adsorption with Brunauer-Emmett-Teller (BET), Scanning Electron Microscopy (SEM) coupled with Energy Dispersion Spectroscopy (EDS) analyses. XRF analysis shows that cations and aluminum were removed due to pre-treatments and that the clinoptilolite, with a smaller particle size, had a higher Si/Al ratio. All clinoptilolites showed good thermal stability up to temperatures 600–800 °C with continuous mass-loss curves. It was determined that surface area and total pore volume increased in most of the samples without agglomeration by SEM-EDS and BET. The surface functional groups were investigated by FTIR and intensities of some bands showed a decrease due to decationization.

Keywords: Clinoptilolite, acid treatment, calcination, natural zeolite, heat treatment.

Submitted: March 29, 2022. **Accepted:** June 13, 2022.

Cite this: Bayrakdar Ates E. Investigating the Chemical and Thermal Based Treatment Procedures on the Clinoptilolite to Improve the Physicochemical Properties. JOTCSB. 2022;5(2):39–58.

***Corresponding author. E-mail:** ezgi.bayrakdar@yalova.edu.tr.

INTRODUCTION

Zeolites consist of various minerals and have great scientific and industrial applications in different areas. The larger surface area of zeolites due to porosity and their high thermal strength make them frequently preferred materials for different applications, especially adsorbents, catalysts (1-3), the water purification (4-6), microelectronics, optics, medicine, and agriculture. The most important features that make it a material that can be used in many different areas are listed as high adsorption ability, molecular sieve capacity, high selectivity, ion exchange capacity, strong resistance to acidic substances, and high thermal resistance (7). Zeolites are called hydrated aluminosilicates containing silicon and aluminum atoms bonded to each other with oxygen atoms, arranged in crystal structure and tetrahedral units, with a three-dimensional structure, which is generally characterized as natural or synthetic zeolite, with channels and spaces formed due to the microporous surface structure (1,7-12). The most important feature that distinguishes zeolite from other crystal structures and aluminosilicate-based materials is the presence of structural voids connected to each other by channels. The structure and size of these voids and channels are different for each zeolite and are considered characteristic features (4,10,13). Each aluminum atom causes one negative charge in the zeolite structure which is generally balanced with an exchangeable cation (Ca^{2+}, Mg^{2+}, Na^{+}, K^{+}, etc). Considering the significant behaviors of the exchangeable cations, they affect the adsorption and thermal characteristics of the zeolites (9). The ion exchange characteristics of zeolite are sourced from exchangeable cations and provide the advantage of using it in many fields (2).

When the literature is examined, it is seen that zeolites, whose aluminum content has been diluted by dealumination, provide important advantages, especially in terms of catalysis. Despite its impurities, it has been determined that these zeolite-based catalysts, which have strict thermal stability, have high selectivity for different catalytic reactions, thanks to the alternatives brought by their chemical content and molecular structure. Compared to metal oxide catalysts, they exhibit higher activity, on the other hand, they are more stable than noble metal-based catalysts. Mesopores in natural zeolite structures provide an advantage in the diffusion of reactants into micropores where active centers occur (10,14-17). Similarly, Król and Jeleń (7) also stated that the inner surface area of the zeolites is large and has more than one active site. This feature of zeolites is especially important in catalytic applications both as a stand-alone catalyst and as catalyst support. Zeolites are usually dealuminated and removal of

cations from the framework by acid (HCl, HNO_3, H_2SO_4, and CH_3COOH) (2-4,9,18-23), steaming (3,10,24) and calcination (3,10,23,25-26). Utilization of an acidic mixture, which consists of phosphoric acid and citric acid, has already been carried out as an alternative (27). The main goal of acid pre-treatment is to remove the aluminum from the zeolite to create more pores in the structure (4,28). When the studies in the literature are examined, it may not be a very simple procedure to improve the properties of zeolite by treating it with acid. Because the types of zeolites can be so diverse, there may be some cases where the application and effect of each pretreatment are not the same for all species (4,19). Simple inorganic salts and alkalis are also used for the pretreatment process, allowing the cations to move away from the structure and increase the nSi/nAl ratio (10).

When both adsorption and catalytic properties of zeolites were examined, it was stated that these properties were not only affected by the type of out-of-frame cations (29) but were also significantly affected by the amount of water in the structure (7,25). When the literature studies are examined, problems are experienced during the use of natural zeolites due to high water demands (25,30-33). Therefore, the application of the calcination process (10,22,25,33-35), as preferred in this study, is of great importance. The high surface area of zeolites due to the porosity originating from micro and mesopores results in an increase in the water demand characteristics. Seraj et al. (25) stated that the high surface area feature of natural zeolites is often due to internal porosity. They explained the high water demand of natural zeolites by accepting that the water was adsorbed into the internal pores (34,36). Seraj et al. (25) stated that if the structure of the pores is changed in a way that prevents water adsorption, there will be a decrease in water demand. For this, they proposed calcination as a thermal pretreatment in the zeolite structure and examined its effect on the structure. It was emphasized that not only the decrease in water demand in the structure after calcination but also a significant improvement in the workability of the material will occur due to this decreasing demand. It has been stated that the calcination process will also be effective in removing the clay impurities that may increase the water demand by absorbing the water in the structure (37). However, Seraj et al. (25), Wang et al. (22) and Ates and Hardcre (3) reported that agglomeration occurred in the structure at high temperatures such as 600, 650, 700, 750, and 800 °C. Perraki et al. (26) explained that the thermal behavior of the zeolite when applied to a heat treatment such as calcination also depends on the amount of Al in its structure. They stated that since clinoptilolite is a zeolite with a Si/Al ratio greater than 4, its thermal resistance is high at temperatures above 450 °C. Considering these different studies, performing calcination and acid pretreatment together is very important in terms of improving the physicochemical properties of the zeolite. Considering these different studies, it is very important to carry out calcination and acid pretreatment together, as the author applied in her study, in terms of improving the physicochemical properties of the zeolite.

Clinoptilolite is one of the most common types of zeolites encountered in nature and is frequently used in different fields (8,12,35,38,39). Clinoptilolite is in the heulandite group and has the highest thermal resistance among the zeolites in this group. When the clinoptilolite structure is examined, it is seen that it consists of two types of channels connected with eight-membered rings (9,38,40-43). Clinoptilolite has a significant cation exchange capacity due to the presence of extra framework cations in its structure (41,42,44,45).

Clinoptilolite generally includes impurities that could differ due to the region of the reserve and these impurities strict its utilization. In the literature, several treatment methods were improved and applied to remove these impurities and enhance the chemical and physical properties of different zeolite types. Clinoptilolites are widely used for catalytic and adsorption purposes as important structural properties such as surface area, total pore volume, pore diameter, chemical structure, water content, and porosity change as a result of pretreatment (8,9,46,47). The low cost of clinoptilolites has also been an important reason for their use for adsorption (9,48), environmental applications (48-50), and catalysts (43). With the removal of cations from the structure of clinoptilolites, which are pre-treated with acid, the voids formed in the structure increase the specific area and surface, and new acidic regions appear. While this situation changes the adsorption characteristics of the zeolite, on the other hand, if it is to be used as a catalyst instead of an adsorbent, the increased surface area causes an increase in both the catalytic activity and the selectivity of the products (41,52).

In this study, the effect of different calcination temperatures (300 and 500 °C) on two different clinoptilolite samples (with different particle sizes), as well as varying durations of calcination (2 and 3 h), were investigated after pretreatment with hydrochloric acid. Burris and Juenger (34) stated that the literature focused on examining the effect of calcination on zeolites used in cementitious mixtures compared to clinoptilolite. Therefore, this study is important not only in terms of the effects of pretreatment of clinoptilolite with calcination in the literature but also in terms of comparing the effects of different calcination temperatures and durations on clinoptilolite samples with different particle sizes. With the characterization tests, it is possible to compare the samples calcined at the same temperature and time, pre-treated at the same acid concentration, in terms of different particle sizes at the beginning, on the other hand, the effect of the changing pretreatment conditions on the physicochemical properties in the same sample was investigated. At the same time, considering the contribution of the acid and pre-treatment applied before the calcination process together with the calcination, as stated before, to the structure, it is seen that it has an important contribution to the improvement of the properties of the structure, especially by removing impurities. Although it is stated in the literature that calcination may cause surface agglomeration and sintering problems, especially if the calcination temperatures are selected high, it is clearly seen that the preferred temperatures in this study do not cause agglomeration in the structure, as supported by SEM analysis. In this case, it has been determined that the pretreatment with HCl applied before calcination is also important. When the obtained characterization results were examined, possible changes in the structure (change in cation concentration, dealumination, change in peak densities, etc.), especially after acidic pretreatment, were in line with the literature. In addition, as stated in the article, not using a high concentration of the acidic solution and sufficient contact time did not damage the crystalline structure, morphological features, and other characteristic features related to the structure. Burris and Juenger (34)

stated that the calcination temperature values recommended by the researchers vary according to the zeolite type and the optimum calcination detection scale, in other words, there is no single truth in this regard. From this point of view, it is thought that this study on clinoptilolite, in which fewer calcination effects are investigated, will make significant contributions to the literature. In addition, not many studies have been found in which the effect of calcination time has been examined together with the parameter of being a natural clinoptilolite obtained from the same region but having different particle sizes.

MATERIALS AND METHODS

Raw Materials and Reagents

Natural clinoptilolite samples from Gordes were used, supplied by Gordes Zeolite Mining Corporation. These clinoptilolite samples particle size are 50 μ (Clinoptilolite-A) and 150 μ (Clinoptilolite-B), respectively. The mineral acid, HCl (≥ 37%), was supplied by Merck (Darmstadt, Germany) and all solutions were prepared by using deionized water.

Pre-treatment Procedure for Natural Clinoptilolite

The procedure of the pre-treatment of natural clinoptilolites is shown in Figure 1. A required amount of the clinoptilolite was put into deionized water and stirred for 24 h using a magnetic stirrer in a three-neck round-bottomed flask at 30 °C. In the pre-treatment method, after the pre-mixing period, the clinoptilolite sample was filtered under vacuum and dried in a furnace at 105 °C for 2-3 hours. The HCl solution concentrations were fixed at 0.3 M and, these dried natural zeolite samples were wetted and stirred with HCl solution at 52 °C for 1 hour. According to preliminary experiments, the HCl solution amount was fixed at the optimum ratio of HCl solution/Clinoptilolite (v/w) 10:1. The acid-pre-treated sample was separated by centrifugation, then washed by using excess deionized water until the pH is 7 and then dried at 105 °C in a furnace for 2-3 h. The samples obtained were calcinated at 300 and 500 °C for both 2 and 3 h.

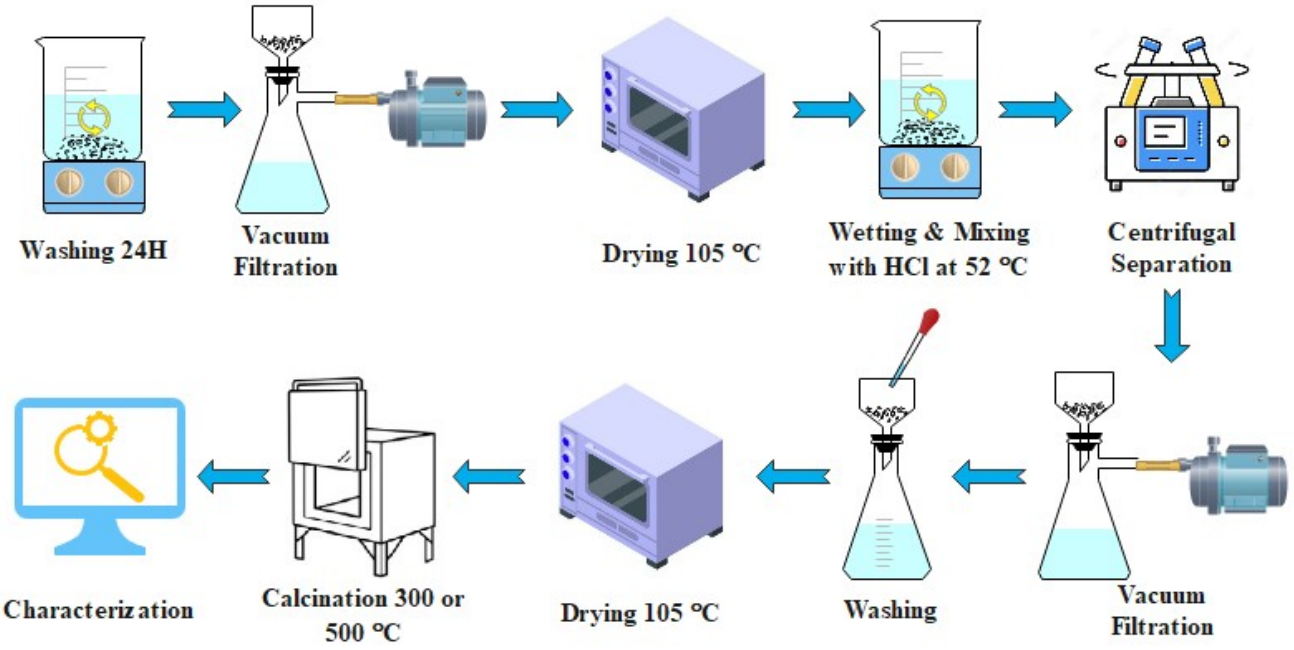

Figure 1: Procedure of the pre-treatment of natural clinoptilolites.

The pre-treated clinoptilolite samples belonging to (Clinoptilolite-A) were denoted as Clinoptilolite-A_1, Clinoptilolite-A_2, Clinoptilolite-A_3 and Clinoptilolite-A_4, according to their corresponding 300°C for 2 h, 300°C for 3 h, 500°C for 2 h and 500°C for 3 h calcinations, respectively. In the same way, other pre-treated natural zeolite samples prepared from (Clinoptilolite-B) were named as Clinoptilolite-B_1, Clinoptilolite-B_2, Clinoptilolite-B_3 and Clinoptilolite-B_4, calcined at 300°C for 2 h, 300°C for 3 h, 500°C for 2 h and 500°C for 3 h, respectively.

Characterization

The chemical compositions of the natural clinoptilolite samples were determined on powdered samples with X-ray fluorescence (XRF, Spectro Xepos II).

X-ray powder diffraction (XRD) patterns of zeolites were recorded on a Panalytical Empyrean diffractometer using nonmonochromotografic Cu Kα1-radiation (45 kV, 40 mA, k = 1.5 Å). The scanning range was 4–90°/(2θ) and with an incremental step size of 0.02° 2θ and 2 s dwell time. Thermal behaviors were investigated using a Seiko, TG/DTA 6300 instrument (range: 25-900°C) under flowing nitrogen (150 mL min^{-1}) at a heating rate of 10 °C min^{-1} using approximately 5-5.5 mg of clinoptilolite samples in alumina crucibles. Physisorption isotherms were determined by the adsorption of N_2 at 77 K in a OANTACHROME AUTOSORB IQ2. High purity (99.99%) nitrogen was used in the adsorption measurements. The clinoptilolite samples were previously heated at a temperature of 160 °C under vacuum for 12 h to remove the volatile compounds in the structures, to provide more gas adsorption to the surfaces, and determine the surface area and pore size distributions more accurately. The pore size distributions and specific surface area of samples were calculated by the Barrett–Joyner–Halenda (BJH) and BET

methods, respectively. Infrared absorption measurements of the clinoptilolite samples were obtained using a Fourier transform infrared (FTIR) spectrometer (PERKIN ELMER-SPECTRUM 100). The FTIR spectra were recorded in the wavenumber range of 400–4000 cm^{-1} at a resolution of 4 cm^{-1} with the use of ATR technique. The morphological structures and elemental distributions were investigated by using scanning electron microscopy (SEM) with a JEOL Brand JSM 6610 model used with a system for elemental composition and elemental mapping analysis based on energy-assisted X-ray spectroscopy (EDS) system (Oxford Instruments Brand, Inca X-act model). Before the beginning of the SEM analysis, to provide the conductivity of all-natural and treated clinoptilolites, the surface of the samples (Quorum brand, SC-7620 model) was coated with argon gas environment for nearly 150 seconds with 99% purity gold (Au) at an approximate thickness of 200 angstroms. Images of the sample surfaces were recorded for different magnifications at an accelerating voltage of 15 kV in a vacuum, spot size of 30, and a working distance of approximately 12 mm. Elemental analysis was carried out for different points randomly determined on the clinoptilolite surfaces and the average of those found was shown.

RESULTS AND DISCUSSION

Elemental Composition (XRF Analysis)

The XRF analyses of the natural (Clinoptilolite-A and Clinoptilolite-B) and that of pre-treated (Clinoptilolite-A_1, Clinoptilolite-A_1, Clinoptilolite-A_1, Clinoptilolite-A_1, Clinoptilolite-B_1, Clinoptilolite-B_2, Clinoptilolite-B_3 and Clinoptilolite-B_4) samples of clinoptilolites are presented in Table 1. The elements located at smaller concentrations compared to Al and Si were determined and recorded in oxide form. The XRF element analysis resulted in a significant amount of silicon (Si) in all of the samples (Table 1). It was found that SiO_2 concentrations showed a significant increase following the acid and calcination treatments. Both acid and calcination treatments did not cause any critical destruction of the crystal lattice in comparison with the natural clinoptilolites. The natural clinoptilolite samples (Clinoptilolite-A and Clinoptilolite-B) were quantified by the high amounts of potassium and calcium while magnesium, sodium, and phosphorus amounts are low. Additionally, iron is determined as iron oxides. According to Table 1, treatment of both acid-treated-clinoptilolites with increasing calcination temperature and calcination period resulted from the subtraction of cations (Ca^{2+}, Mg^{2+}, and K^{+}) from the samples. Although the findings on cation concentrations are correlated to literature (2,3,9,10,43,48,53,54), two different types of zeolites and their pretreated samples showed different behaviors in dealumination. With increasing calcination temperature and duration, aluminum oxide concentration had a decreasing trend for Clinoptilolite-A and pre-treated samples except for Clinoptilolite-A_1. Radosavljević-Mihajlović et al. (53) emphasized that a movement to framework could happen and dealumination takes place when the acid solution concentration is above 0.1 M (0.3 M acid solution used in this study) at treatment. Conversely, Clinoptilolite-A samples, small increases in aluminum oxide concentrations were observed for the four of the treated Clinoptilolite-B samples. This decreasing trend (for Clinoptilolite-A and its treated versions) and the increasing trend (for Clinoptilolite-B and its treated versions) showed a slightly reverse trend with the increase in time at the same calcination temperatures. Elaiopoulos et al. (10) explained the unexpected dealumination problems as the existence of huge (hydrated) and effectively involved in ion-exchangeable cations at K3 (in the center of distorted 8-member rings) might prevent Al^{3+} motion. Further dealumination could not be performed due to the other factor being the exposure of the acid-treated zeolite samples to high temperatures. While this high-temperature value was 700 °C in their study, the dealumination of all Clinoptilolite-B samples treated at both 300 and 500 °C in this study was below the expectation mentioned before. Additionally, Davarpanah et al., (41) and Sato et al. (55) explained that negligible change in Al content is correlated to dealumination coming true in the exchange (55). Miądlicki et al. (43) also indicated that an effective increase in dealumination could be determined with alkali pH values of the treatment solution. In higher acidic pH values such as above 0.1 M, dealumination could slightly occur as in our study.

X-Ray Diffraction (XRD) Analysis

The XRD patterns of the natural and acid-treated resultant products (Clinoptilolite-A, Clinoptilolite-A_1, Clinoptilolite-A_2, Clinoptilolite-A_3, Clinoptilolite-A_4) exposed with a varying calcination temperature and time for thermal treatment are given in Figure 2, and other samples (Clinoptilolite-B, Clinoptilolite-B_1, Clinoptilolite-B_2, Clinoptilolite-B_3, Clinoptilolite-B_4) prepared with the same treatment procedure and conditions are given in Figure 3. The natural clinoptilolite XRD spectrum was correlated to the literature. The XRD graphics had typical peaks of clinoptilolite, according to JCPDS card 25–1349, for natural and acid-treated clinoptilolites (2θ = 9.85°, 11.19°, 13.09°, 16.92°, 17.31°, 19.09°, 20.42°, 22.48°, 22.75°, 25.06°, 26.05°, 28.02°, 28.58°, 29.07°, 30.12°, 31.97°, 32.77°). The other four peaks (2θ = 20.86°, 26.6°, 36.55°, 39.45°) according to JCPDS card 85–0930 belonged to quartz, which is an impurity phase in natural clinoptilolite.

There are changes in XRD peak sharpness and intensity in all treated types of Clinoptilolite-A and all B-type clinoptilolites. It was clear that XRD patterns of the acid and temperature treated clinoptilolites clearly show differences in regard to both natural clinoptilolites. These differences, such as the sharpening of some peaks, enhanced due to higher calcination temperatures and time for especially Clinoptilolite-B and its treated ones in Figure 3. Compared to Clinoptilolite-A_3 and Clinoptilolite-A_4 samples, the intensity of the peaks of Clinoptilolite-A_1 and Clinoptilolite-A_2 samples (calcination temperature: 300 °C) are so near to Clinoptilolite-A. It was determined that intensities of clinoptilolite peaks show a decline with increasing calcination temperature for Clinoptilolite-A_3, Clinoptilolite-A_4, Clinoptilolite-B_3, and Clinoptilolite-B_4. The change in calcination time did not cause a great change in the clinoptilolite structure, at the same calcination temperatures for all treated clinoptilolites. However, it resulted from both XRD patterns that higher calcination temperature (500 °C) and longer calcination time at this temperature affect the crystal structures of all treated clinoptilolite samples compared to natural clinoptilolites and samples pretreated at lower calcination temperature (300 °C). The relative crystallinity of the clinoptilolite samples showed a decreasing trend with increasing calcination temperature. Burris and Juenger (34) observed that the changes in clinoptilolite phases due to calcination were so near for all samples as in our study. They also explained that calcination will cause a decrease in crystallinity, which will

be pointed out by a decrease in the heights of the characteristic clinoptilolite peaks. As in our study, a greater decrease was observed for the same peaks with the increase of the calcination temperature, compared to the decrease in the clinoptilolite peaks as a result of the calcination process performed at 300 °C. They also stated that for each clinoptilolite sample, the decrease in clinoptilolite crystallinity due to calcination varied with the increase in the original amorphous amount of the clinoptilolite. Elaiopoulos et al. (38) stated that after the heat treatment was applied at 350 °C, important peak points for zeolite can be greatly affected. Seraj et al. (25) also determined a significant decrease in the intensity of clinoptilolite peaks in the XRD patterns for natural zeolite due to calcination. Florez et al. (35) determined that the amount of amorphous material increased as the calcination process temperature increased according to XRD analysis. They stated that calcination has thermal effects on natural zeolite such as water loss, collapse of the crystal structure and gradual amorphization. In many studies in the literature, a decrease in peak density was observed in zeolite samples pretreated with acid (2,3,22,39,43,56). In other words, the pretreatment carried out with acid also has an effect on the changes in crystallinity and peak densities in this study.

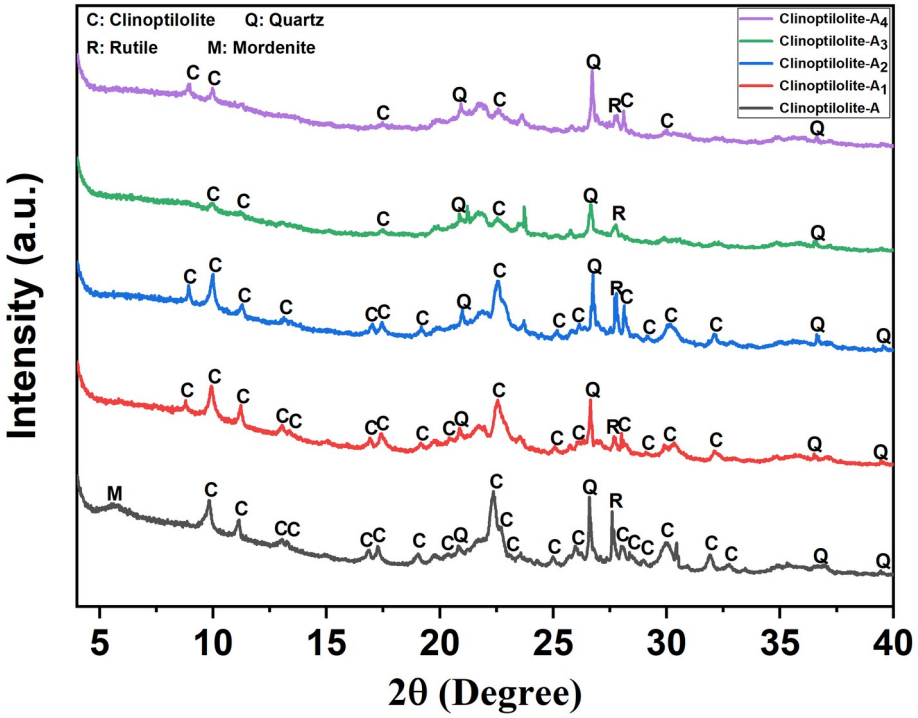

Figure 2: Typical peaks of the Clinoptilolite-A and acid-treated resultant products determined with XRD pattern.

Table 1: Chemical compositions (wt%) and SiO_2/Al_2O_3 ratios of natural and pretreated clinoptilolites determined by using XRF analysis.

Sample	SiO_2	Al_2O_3	Fe_2O_3	CaO	MgO	K_2O	Na_2O	P_2O_5	SrO	TiO_2	SiO_2/Al_2O_3
Clinoptilolite-A	79.37	13.88	1.305	2.437	1.963	2.491	1.26	0.04	0.05	0.09	5.71
Clinoptilolite-A_1	81.8	13.97	0.989	1.141	1.808	1.816	1.297	0.01	0.02	0.07	5.85
Clinoptilolite-A_2	82.01	13.34	1.179	1.285	1.718	2.053	1.192	0.01	0.03	0.09	6.14
Clinoptilolite-A_3	81.88	13.1	1.275	1.42	1.669	2.163	1.25	0.01	0.03	0.09	6.25
Clinoptilolite-A_4	81.74	13.38	1.236	1.373	1.686	2.112	1.24	0.01	0.03	0.09	6.10
Clinoptilolite-B	77.87	14.61	1.628	2.426	1.74	3.217	1.198	0.03	0.03	0.09	5.32
Clinoptilolite-B_1	80.64	14.67	1.172	1.243	1.611	2.46	0.979	0.01	0.01	0.09	5.49
Clinoptilolite-B_2	80.48	15.23	1.025	1.086	1.719	2.127	1.16	0.01	0.01	0.06	5.28
Clinoptilolite-B_3	80.8	14.66	1.17	1.225	1.649	2.36	0.924	0.01	0.01	0.07	5.51
Clinoptilolite-B_4	80.62	15.2	1.042	1.076	1.791	2.112	0.959	0.01	0.01	0.08	5.30

Miądlicki et al. (43) indicated that clinoptilolite treated by using an acidic solution at a concentration of higher than 0.1 M (this is 0.3 M in our study) negatively affects the crystallinity of the sample. Considering Wang et al. (2) study, it can be explained that the changes in the 9.85 and 22.48°2θ peaks in the XRD patterns in this study were directly caused by the acidic treatment. This situation is explained by dealumination from the structure of clinoptilolite as a result of acid treatment. In our study, there was no significant change in the intensity of quartz peaks for treated Clinoptilolite-A and Clinoptilolite-B samples. Wang et al. (2) stated that the structure of quartz changes and its crystallinity decreases when the zeolite is pretreated with alkali, not by pretreatment with acid (54). Kim et al. (57) found that clinoptilolites were more durable than heulandites (HEUs) despite high-temperature heat treatment and acid pretreatment.

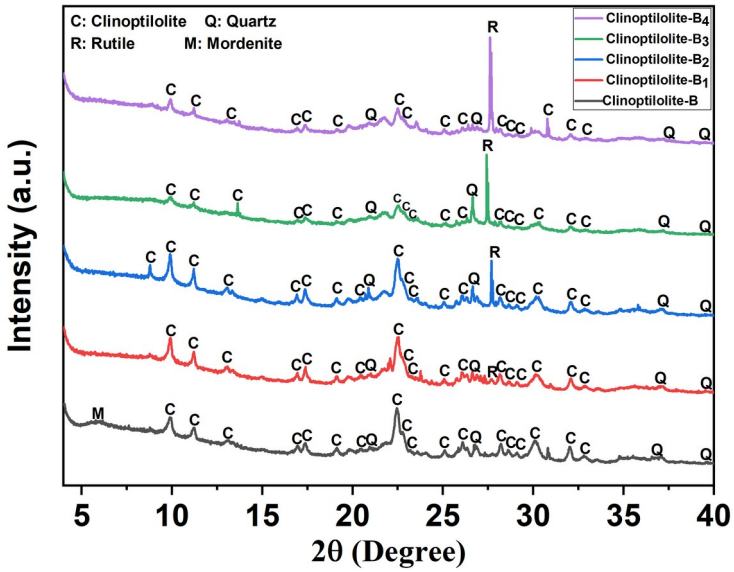

Figure 3: Typical peaks of the Clinoptilolite-B and acid-treated resultant products determined with XRD pattern.

Fourier Transform Infrared Transmittance Spectra (FT-IR) Analysis

FT-IR spectra could be used to put forth the structure of zeolite samples. The FTIR spectra of the natural and treated clinoptilolites investigated between the 400–4000 cm^{-1} wavenumber are given in Figure 4 (Clinoptilolite-A, Clinoptilolite-A_1, Clinoptilolite-A_2, Clinoptilolite-A_3, Clinoptilolite-A_4) and Figure 5 (Clinoptilolite-B, Clinoptilolite-B_1, Clinoptilolite-B_2, Clinoptilolite-B_3, Clinoptilolite-B_4). The exact points of the bands determined in every clinoptilolite are given in Table 2 (3,9,10,38,43,54,56).

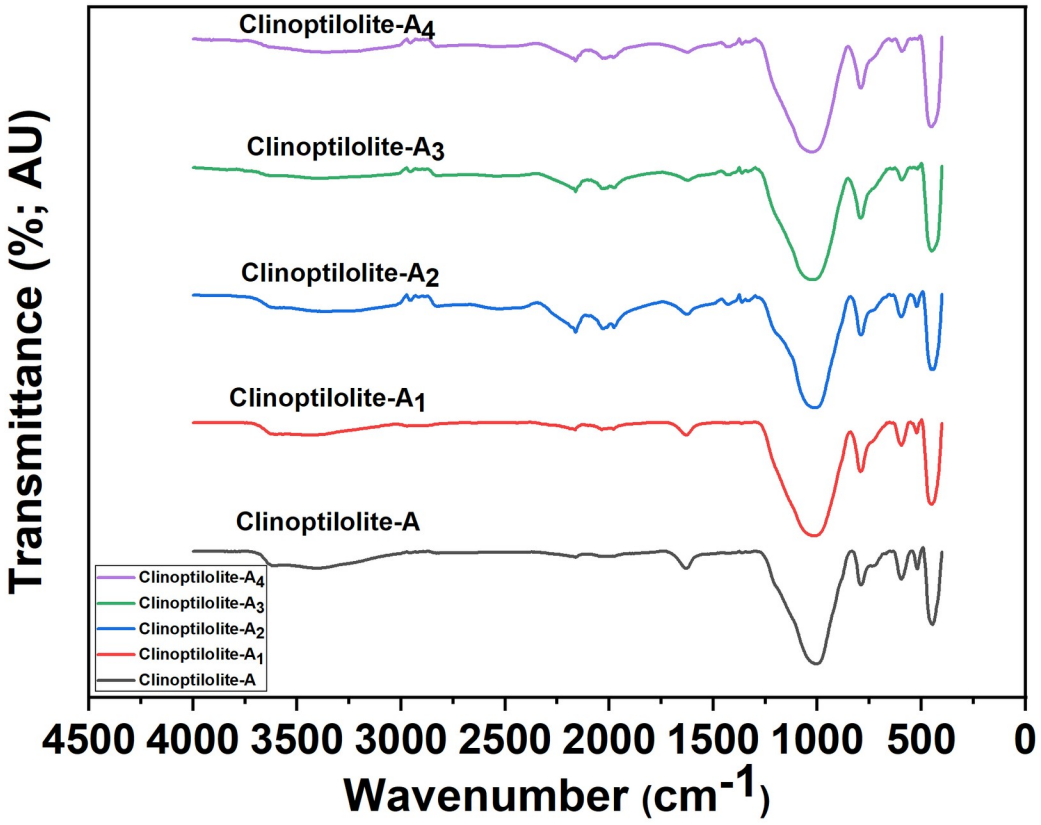

Figure 4: The FT-IR spectra of the Clinoptilolite-A and acid-treated resultant products.

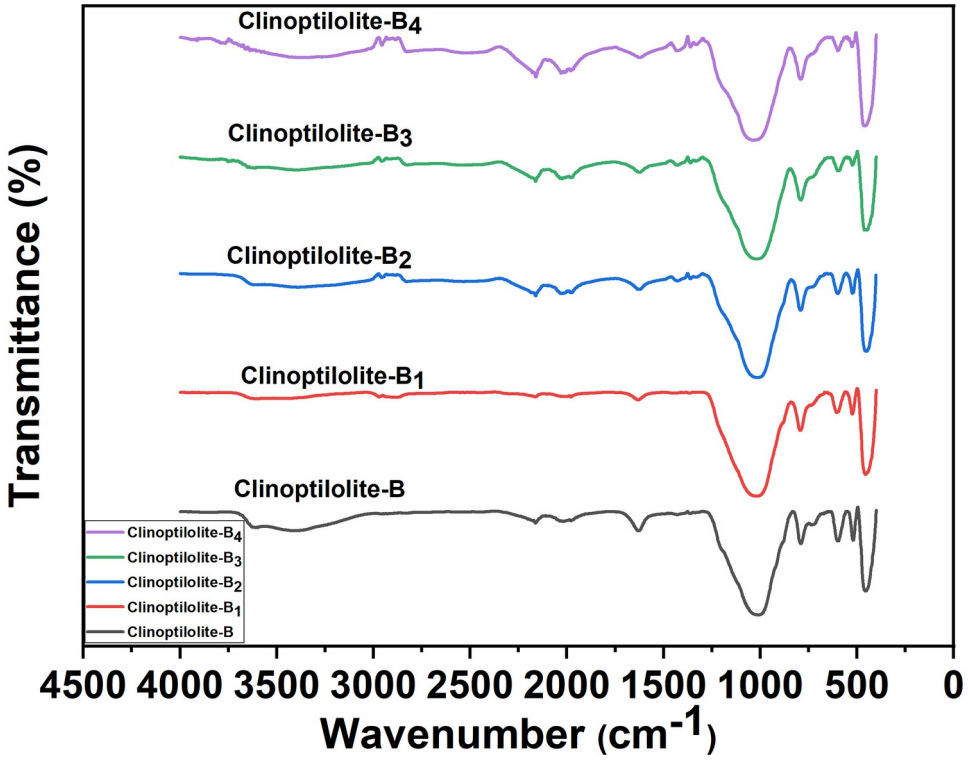

Figure 5: The FT-IR spectra of the Clinoptilolite-B and acid-treated resultant products.

Table 2: The peak wavenumber of bands determined in FT-IR analysis for natural and pretreated clinoptilolites.

Sample	T-O stretching vibration		T-O bending vibration	OH^- Stretching	OH^- Bending and/or NH_3	Other
	Zeolite	SiO_2				
Clinoptilolite-A	1004	790.58	446.91	3611.30, 3414.74	1629.41	595.97, 519.16
Clinoptilolite-A_1	1015.22	792.21	448.33	3432.05	1629.85	595.76, 522.66
Clinoptilolite-A_2	1010.97	790.66	442.77	3385.35,	1625.62,1430.99, 1362.37, 1331.90	597.18, 523.28
Clinoptilolite-A_3	1023.97	792.28	450.63	3392.38	1621.85, 1434.79, 1361.88	595.46
Clinoptilolite-A_4	1026.81	791.11	453.05	3362.40	1627.88, 1428.70, 1361.25	641.40, 593.16
Clinoptilolite-B	1009.52	789.87	456.02	3610.41, 3415.86	1629.90	596.28, 519.52
Clinoptilolite-B_1	1021.03	793.04	455.94	3610.17	1629.96	524.50, 604.98
Clinoptilolite-B_2	1015.25	791.12	451.09	3388.05	1628.15, 1428.01, 1361.43	599.31, 523.12,
Clinoptilolite-B_3	1019.23	790.25	459.01, 447.28	3393.73	1623.05, 1427.09, 1361.63	598.52, 523.83
Clinoptilolite-B_4	nd	789.11	460.25	3911.41, 3765.89, 3372.64	1626.06, 1431.03, 1360.39, 1330.25	599.86, 525.97

The characteristic bands in the range of 1600–3700 cm^{-1} could be attributed to the water in clinoptilolite. According to Bilgiç (1), while the (4000-3000 cm^{-1}) region in the FTIR spectrum indicates the presence of various OH groups, hydroxyl vibrations are observed in this region. Figure 4 and Figure 5 indicate three characteristic bands appearing in the spectra of all samples, at ∼3414 cm^{-1}, ∼3610 cm^{-1}, ∼3910 cm^{-1}, ∼3765 cm^{-1} and ∼3380 cm^{-1}. The band at 3910 cm^{-1} is correlated to isolated silanol groups (Si–OH), the band at ∼3414 cm^{-1} is sourced from Si–O(H)–Al, and the band at ∼3414 cm^{-1} is assigned to hydrogen bonded Si–OH groups in nest deformities and hydrogen bonding of slouching kept water molecules (3,10,38,43,54,58-60). Isolated OH stretching at 3611.30 cm^{-1} for Clinoptilolite-A, 3610.41 cm^{-1} for Clinoptilolite-B and at 3610.17 cm^{-1} for Clinoptilolite-B_1 was determined due to the interplay among the water hydroxyl and cations. Due to acid and heat treatments, the intensity of this band showed a decrease in all treated samples as a result of decationization and dealumination from the structure (3,10,61,62). Another bands are assigned to the hydrogen bonding in the water structure to surface oxygen (3414–3416 cm^{-1}) and to the bending mode of water molecules (∼1629 cm^{-1}) (3,43,38,56). The bands at 1400–1450 cm^{-1} could be attributed to NH_3 bound by Bronsted sites (10,56). Bilgiç (1) also determined a band at 1398 cm^{-1} which belongs to NH_4^+. Bands in the 1300-1450 cm^{-1} wavelength range were not observed in natural clinoptilolites, Clinoptilolite-A_1, and Clinoptilolite-B_1 samples, but were observed in Clinoptilolite-A_2, Clinoptilolite-A_3, Clinoptilolite-A_4, Clinoptilolite-B_2, Clinoptilolite-B_3, Clinoptilolite-B_4 samples that were calcined at the same temperature for a longer time or whose calcination temperature was increased.

In the range of 1600–1450 cm^{-1}, there are not extended bands and they are assigned to the bending mode of water. In this study, however, these bands were not determined in the all- natural and treated clinoptilolites. Ates and Hardacre (3) also stated that these bands could be determined in slight transmittance or not existing for the treated samples. For the wavenumber 600–800 cm^{-1}, the bands are assigned to pseudo-crystallinic vibrations (3,54,63). In this interval; there is an intensity for the band at 789–794 cm^{-1} which is assigned to Si-O stretching in all-natural and treated samples (3,43,51,54,60,64). This band is also sourced from amorphous silica or the opal CT-like phase generated with the zeolite phase solvation due to the treatments (3,51). The Si–O stretching vibrations of Clinoptilolite-A and Clinoptilolite-B are being moved to a higher wavenumber after acid and heat treatment. The band detected at near ∼794 cm^{-1} for Clinoptilolite-B_1 could be assigned to quartz or amorphous SiO_2, which is confirmed by the XRD pattern and XRF analysis (54).

The dominant T–O stretching vibration bands are detected in the 1045–1070 cm^{-1} region. The intensity of this band is proportionated with the Si/Al ratio (3,10,43,54). When the more Al^{3+} atoms are removed from the clinoptilolite structure, this band is expected to give higher wavelengths in the FTIR spectra from ∼1047 cm^{-1} onwards. However, it was stated that samples with a high Al^{3+} amount gave bands around ∼1022 cm^{-1} in some studies (10,38,43,54,56,57,60,66). They also explained that the force constant for the mode in the Al-O-Si bond is lower than the corresponding mode in a Si-O-Si bond because the bond between Al-O is weak and longer. This situation causes the wavelength of the clinoptilolite to be lower in these mentioned ranges if the Al^{3+} content is high. In line with this, the bands detected in the range of 1016–1022 cm^{-1} belong to stretching vibrations of the T-O band in Miądlicki et al. (43) study. In the author's study, it was determined that it gave bands in the range of ∼1004-1024 cm^{-1}, which is close to these band gaps but at a lower wavelength range. This is due to the fact that the dealumination could not be achieved at the desired rates, as supported by XRF analyses, and therefore the amount of Al^{3+} present in the structure was higher than the target. However, an increase in the ratio of Si/Al in structure content carries the bands to

higher wavenumbers for especially Clinoptilolite-A_1, Clinoptilolite-A_2, Clinoptilolite-A_3, Clinoptilolite-A_4, Clinoptilolite-B_1 compared to natural clinoptilolites in this study. Compared to Clinoptilolite-B, incremental slip of wavenumbers in Clinoptilolite-B_2 and Clinoptilolite-B_3 could be explained by higher calcination time and calcination temperature, respectively. However, when evaluated in itself, the lower wavelength of the Clinoptilolite-B_2 and Clinoptilolite-B_3 samples compared to Clinoptilolite-B_1 may be due to the longer calcination time in the Clinoptilolite-B_2 sample compared to Clinoptilolite-B_1, and the fact that the Clinoptilolite-B_3 sample calcination was carried out at the same time but at a higher temperature than Clinoptilolite-B_1. In addition to all these, as given in other researches, all possible structures due to the presence of feldspars and amorphous species in non-high purity clinoptilolite samples may cause a wide peak formation in the 1250-850 cm^{-1} region, which prevents determining the exact position of other important bands (10,56,63,65,67,68).

The band in ~437-470 cm^{-1} region could be assigned to Si–O–Si or T-O bending band as mentioned in several studies (10,38,41,54). The band intensity showed differences from structure to structure, pointing out that there is a possibility of overlapping from bands assigned to amorphous structures and/or exchangeable cations. Compared to Clinoptilolite-A_1, Clinoptilolite-A_2, Clinoptilolite-B_1, and Clinoptilolite-B_2; higher wavelength values were determined in this range for Clinoptilolite-A_3, Clinoptilolite-A_4, Clinoptilolite-B_3, and Clinoptilolite-B_4 samples that were pretreated with a higher calcination temperature and longer time. This can be explained by the change in the state of the amorphous structure and exchangeable cations as a result of pretreatment with acid and calcination.

The bands at 519.16 (at Clinoptilolite-A), 522.66 (at Clinoptilolite-A_1), 523.28 (at Clinoptilolite-A_2), 519.52 (at Clinoptilolite-B), 523.12 (Clinoptilolite-B_2), 523.83 (Clinoptilolite-B_3), and 525.97 (Clinoptilolite-B_4) are attributed to extra-framework cations in the structures of samples (41,58). According to these studies in the literature, since these cations are removed in the samples treated by acid solutions with a concentration of 0.5 M and above, no band is observed in this wavelength range, while these bands are existence in the FTIR spectrum of samples pretreated by an acidic solution with a concentration of less than 0.5 M. The weak band determined at 604.98 cm^{-1} in Clinoptilolite-B_1 belongs to bending vibrations among tetrahedra, especially to double ring vibrations (41). Korkuna et al. (56) also stated that the bands detected between 500-700 cm^{-1} belong to pseudo-lattice vibrations in the structure.

Thermogravimetry and Differential Thermal Analysis (TGA-DTA) and Thermal Characteristics

TGA and DTA results are given in Figure 6 (Clinoptilolite-A, Clinoptilolite-A_1, Clinoptilolite-A_2, Clinoptilolite-A_3, Clinoptilolite-A_4) and Figure 7 (Clinoptilolite-B, Clinoptilolite-B_1, Clinoptilolite-B_2, Clinoptilolite-B_3, Clinoptilolite-B_4). Clinoptilolite (natural and treated) had high thermal stability (up to temperatures 600–800 °C) (4,34,48) and showed continuous mass-loss curves as a function of temperature up to 600 °C. The main structural changes, due to especially water loss, occured at temperatures below or around 300-400°C. Therefore, weight loss (%) of the natural and pretreated clinoptilolites determined using TGA-DTA analysis at different temperature ranges up to 600 °C are shown in Table 3. The major amount of water in the clinoptilolite structure could be removed by heating at temperatures lower than 450 °C without damaging the structure (7,34,38,48,54,56). Additionally, when the TG curves were examined, it was stated that they showed a regular weight loss up to 700 °C due to water loss. It has been determined that the DTA curves of all treated/untreated clinoptilolites have a strong endothermic effect at ~350 °C. It is correlated to the removal of physically adsorbed water. In literature, different researchers (48,56,69) determined the endothermic effects in the DTA curves due to the removal of water up to 200°C.

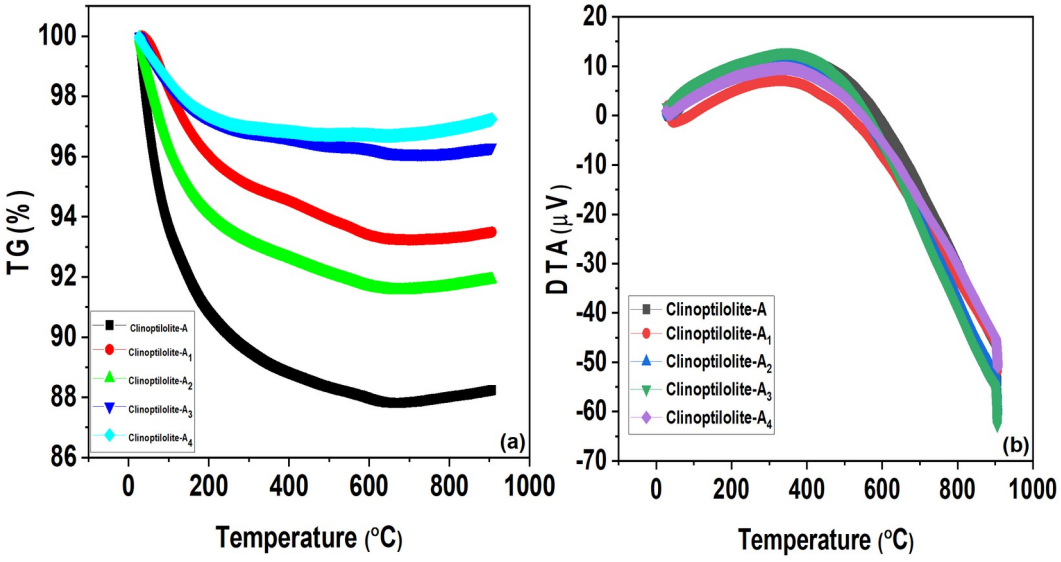

Figure 6: Comparison of thermal behaviors due to (a) TGA and (b) DTA of the Clinoptilolite-A and acid-treated resultant products.

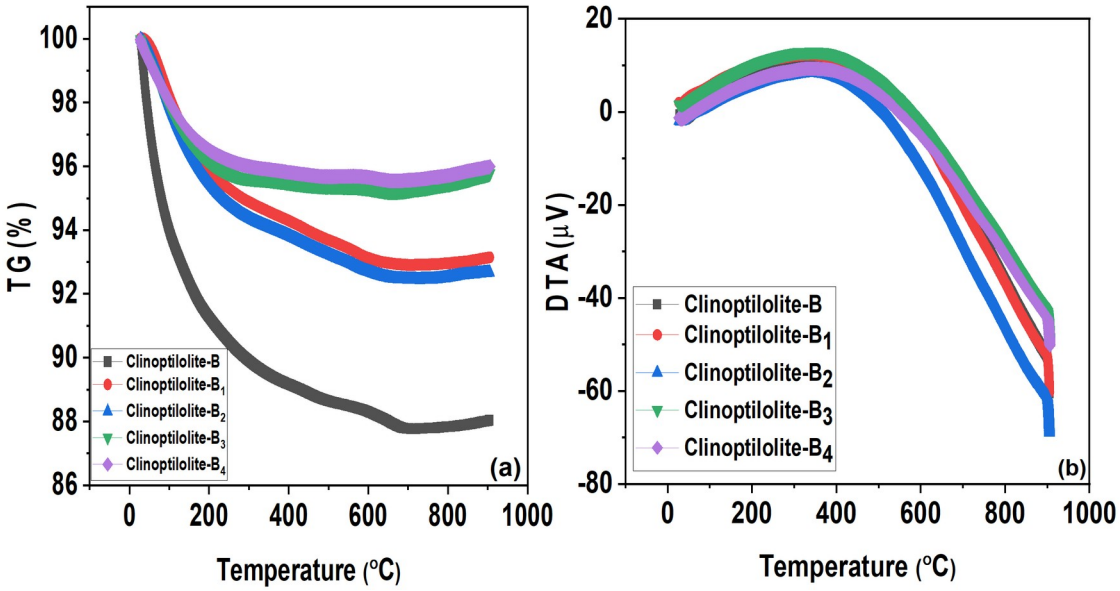

Figure 7: Comparison of thermal behaviors due to (a) TGA and (b) DTA of the Clinoptilolite-B and acid-treated resultant products.

Table 3: Weight loss (%) of the natural and pretreated clinoptilolites determined using TGA at different temperature ranges.

Sample	Weight Loss % 30-100°C	Weight Loss % 100-200°C	Weight Loss % 200-300°C	Weight Loss % 300-400°C	Weight Loss % 400-500°C	Weight Loss % 500-600°C	Total
Clinoptilolite-A	6.327	2.832	1.297	0.731	0.476	0.369	12.032
Clinoptilolite-A_1	1.746	2.209	0.997	0.517	0.597	0.541	6.607
Clinoptilolite-A_2	3.582	2.278	0.96	0.551	0.504	0.436	8.311
Clinoptilolite-A_3	1.623	1.125	0.437	0.197	0.236	0.119	3.737
Clinoptilolite-A_4	1.777	1.388	0.403	0.056	0.099	0.004	3.727
Clinoptilolite-B	5.999	2.73	1.368	0.733	0.525	0.34	11.695
Clinoptilolite-B_1	1.764	2.308	1.037	0.593	0.604	0.563	6.869
Clinoptilolite-B_2	2.099	2.42	1.103	0.554	0.58	0.546	7.302
Clinoptilolite-B_3	2.149	1.71	0.521	0.14	0.111	0.07	4.701
Clinoptilolite-B_4	1.977	1.509	0.514	0.192	0.132	0.018	4.342

Decationization and dealumination of pre-treated clinoptilolites, which is supported by the results of XRF analysis, cause a decrease in the hydrophilic characteristics of clinoptilolites. In general, the abundance of the clinoptilolite phase provides a stable structure up to 700 °C. All treatment operations resulted in a decline for clinoptilolite content and removing the cations (especially acid treatment is significant for this), causing higher water removal (22,48,70). When weight loss (%) was totally examined, the weight loss values decreased inversely with the increase of calcination temperature and calcination time applied to both acid-treated clinoptilolite species. Among the pretreated samples, the highest total weight loss was observed in Clinoptilolite-A_2 and Clinoptilolite-B_2 samples, which had the lowest calcination temperature and time, while the lowest total weight loss was detected in Clinoptilolite-A_4 and Clinoptilolite-B_4 samples. When examined in general, the weight loss of Clinoptilolite-B_1, Clinoptilolite-B_3 and Clinoptilolite-B_4 samples are higher than that of pretreated Clinoptilolite-A samples, except for the Clinoptilolite-B_2 sample. This could be explained by the fact that the high Si/Al ratio observed in the pre-treated Clinoptilolite-A samples, as seen in the XRF analysis results, ensures the preservation of the crystal structure (54).

The weight loss in samples exposed to temperatures between 30–100 °C occurs as a result of the desorption of physisorption water. The results differ according to the type of zeolite, acid treatment, calcination temperature and calcination time: Clinoptilolite-A_2> Clinoptilolite-B_3> Clinoptilolite-B_2> Clinoptilolite-B_4> Clinoptilolite-A_4> Clinoptilolite-B_1> Clinoptilolite-A_1> Clinoptilolite-A_3. For all treated Clinoptilolite-A samples, weight loss was greater at

longer duration of calcination at both calcination temperatures. The decrease in weight loss also depends on the decrease in water absorption due to acid pretreatment, as indicated in Ates and Hardacre (3) and Elaiopoulos et al. (38).

Between 100-200 °C, for both clinoptilolite types, the highest weight loss was observed in the samples that were calcined at 300 °C for 3 hours (Clinoptilolite-A_2 and Clinoptilolite-B_2). When calcined at 500 °C, the weight loss decreased due to the increasing calcination time in the acid-pre-treated Clinoptilolite-B_4 sample, while the weight loss increased while the calcination time increased in the pre-treated Clinoptilolite-A_4 sample. The remarkable weight losses for all samples were determined between 30-200 °C due to the removal of physically adsorbed water, the water existing into the clinoptilolite cavities, and cations at the structure (26,48,70).

Compared to the first two temperature ranges, the weight loss values decreased between 200-300 °C. From 200-300 °C, the slope of TG curves started to fall for all samples in Figures 6 and 7 (3,38,48). When examined in itself, it was determined that the weight loss decreased with increasing calcination temperature and calcination time in both clinoptilolite samples. Wang et al. (22) stated that weight loss values decrease due to the increasing calcination temperatures. They also explained that calcination could significantly carry out the removal of water from the surface/structure of zeolites. This indicates that the heat treatment reduces the silanol slot-derived water content in the zeolite structure. Only the Clinoptilolite-B_2 sample showed a slight increase due to the increasing time compared to the other sample calcined at the same temperature in our study.

Weight loss values were less in the range of 300-400 °C. When investigated in itself, it has resulted that the weight loss decreased with increasing calcination temperature and calcination time in both clinoptilolite samples, except for Clinoptilolite-A_2 and Clinoptilolite-B_4. Compared to the first three temperature range values, weight losses were lower between 400-500 °C, as in the temperature range of 300-400 °C. The same situation for the two the temperature range observed in other studies (38,48). The temperature range of 500-600 °C is the range where the lowest weight losses were seen for all treated samples, except for the Clinoptilolite-A_1 sample, and all of the water remaining in the structure was removed during this interval and afterward. The slope of the TG curves was slighter compared to lower temperature ranges (<500°C) (3,34).

According to the examination of analysis results, the water structures that appeared in clinoptilolites could be divided into three versions: physisorbed water (<100 °C), water correlated to extra-framework cations and aluminum (100–400 °C), and water correlated to silanol nests (>400 °C) (22,34).

Brunauer-Emmett-Teller (BET) Analysis

The nitrogen adsorption and desorption isotherms and pore size distributions of natural and pre-treated clinoptilolites are given to explain the structural characteristics of porous samples in Figures 8, 9, and 10. According to the IUPAC (International Union of Pure and Applied Chemistry) classification, the clinoptilolites have Type 4 isotherms with the hysteresis loop. The surface characteristics calculated are shown in Table 4. Zeolites are generally microporous structures, but the primary micropores formed due to the specific crystal structure of the zeolite itself may not be able to reach and adsorb N_2 gas into these pores due to the inhibition of large cations (10,71,72). Due to the acid treatment and calcination, it was determined an increase in the specific surface areas of clinoptilolites (except Clinoptilolite-A_3 and Clinoptilolite-B_1). The increase in surface area and total pore volume as a result of acid pretreatment has been detected in many studies in the literature (2,3,10,22,39,48). These changes in the surface properties such as surface area, micropore volume, and total pore volume could be correlated to removal of the metal cations, dealumination, and some impurities. Pre-treatments cause the generation of defects and voids left by the removed aluminum (2,3,10,22,43,73). Contrary to this, it was stated that adsorption-desorption isotherms are seldomly affected by acid pre-treatment (3). Elaiopoulos et al. (10) stated that it would not be possible to hold all changes in some physicochemical characteristics responsible for the change in the pore structure. Miądlicki et al. (43) also explained that very high acid concentrations above 1 M can damage the crystal structure, resulting in a lower BET surface area and pore volume. This is the reason why the author did not study at very high acid concentration values (used HCI solution concentration was 0.3 M) in the author's study, and the results obtained (except for Clinoptilolite-A_3 and Clinoptilolite-B_1) did not show a decrease in BET surface area and pore volume.

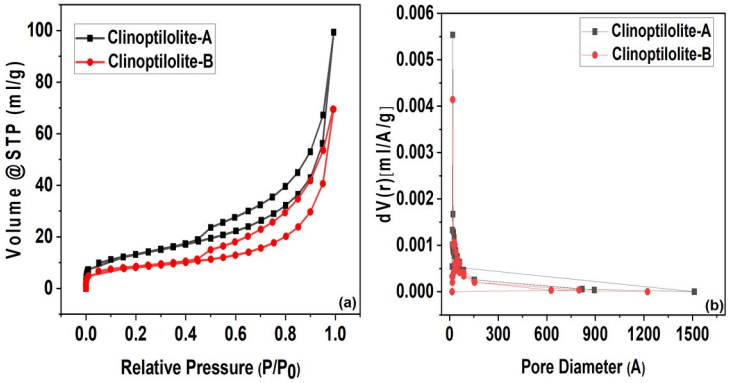

Figure 8: Nitrogen adsorption and desorption isotherms and pore size distributions of Clinoptilolite-A and Clinoptilolite-B according to BET analysis.

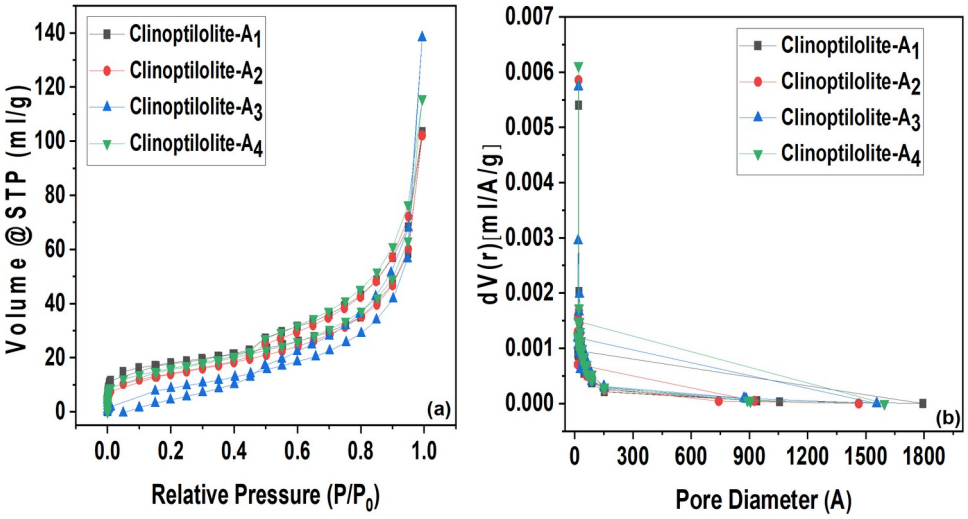

Figure 9: Nitrogen adsorption and desorption isotherms and pore size distributions of the acid-treated clinoptilolites (modified from Clinoptilolite-A) according to BET analysis.

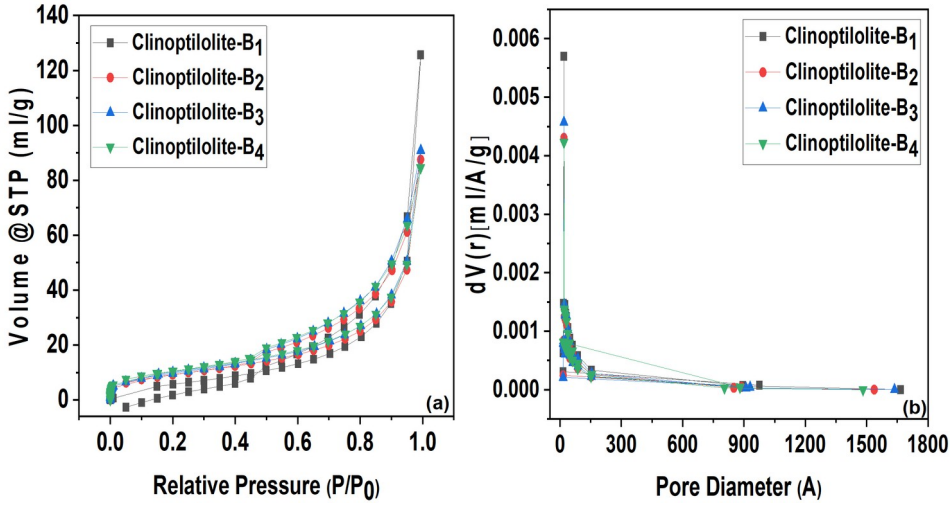

Figure 10: Nitrogen adsorption and desorption isotherms and pore size distributions of the acid-treated clinoptilolites (modified from Clinoptilolite-B) according to BET analysis.

Table 4: Structural parameters calculated for natural and treated clinoptilolites from adsorption–desorption isotherms of nitrogen at 77 K in BET analysis.

Sample	BET Surface Area(m^2/g)	Total pore volume (cm^3/g)	Average Pore Diameter (Å)
Clinoptilolite-A	46.534	0.1538	132.16
Clinoptilolite-A_1	60.318	0.1600	106.06
Clinoptilolite-A_2	49.092	0.1580	128.76
Clinoptilolite-A_3	34.286	0.2140	249.7
Clinoptilolite-A_4	54.594	0.1789	131.1
Clinoptilolite-B	28.246	0.1075	152.26
Clinoptilolite-B_1	26.302	0.1944	295.64
Clinoptilolite-B_2	33.077	0.1355	163.8
Clinoptilolite-B_3	36.037	0.1408	156.24
Clinoptilolite-B_4	36.869	0.1308	141.86

When the pore size distributions of both clinoptilolites (both natural and pre-treated) are examined, it is seen that there is an increase in microporosity due to acid treatment and calcination. This situation can be explained by dealumination due to acid treatment, and it is possible to reach micropores, especially with cations removed from the structure. It was also stated that treatment with acid has a significant effect on pore size distributions (3,9).

When the graphs of both clinoptilolite samples are examined, it is seen that the adsorption values increase, mostly in Clinoptilolite-A_3 and Clinoptilolite-B_1, depending on the increase in relative pressure. Çakıcıoğlu-Özkan and Ülkü (9) also determined this situation in their own studies and stated that the temperature during the HCl pretreatment application was also effective on adsorption. They observed that as this temperature increased, the adsorption decreased especially in the samples that were pretreated with acid at around 100 °C. In our study, no decrease in adsorption values was observed due to the fact that the acid pretreatment application temperature was worked with a value that was almost half of this temperature value.

When the Clinoptilolite-A sample, which was supplied with a smaller pore size, is compared with the Clinoptilolite-B sample with a larger pore size, although the amount of N_2 they adsorbed seems to be close, the Clinoptilolite-A sample adsorbed more N_2 at low pressures as in Figure 8. Similarly, when the pre-treated samples belonging to Clinoptilolite-A were examined in Figure 9, it was determined that Clinoptilolite-A_3 and especially the Clinoptilolite-A_4 sample, which was pretreated by applying a higher calcination temperature, adsorbed more N_2 for lower pressures. When pre-treatment was applied to Clinoptilolite-B, which has larger pores, it was seen that Clinoptilolite-B_2, Clinoptilolite-B_3, and Clinoptilolite-B_4 adsorb N_2 very closely at smaller pressures, but Clinoptilolite-B_4 adsorbs more nitrogen, albeit with a relatively small difference. This situation, especially in the Clinoptilolite-A_4 and Clinoptilolite-B_4 samples, is explained by their lower average pore diameters compared to the diameter of Clinoptilolite-A and Clinoptilolite-B as seen in Table 4. Such a difference was also detected in samples with smaller pore diameters in the Elaiopoulos et al. (10) study, and it was stated that there was too little difference to be seen in the differential pore volume distribution curves. Desorption curves of isotherms show a decrease from P/Po ∼0.45 for Clinoptilolite-A_3 and Clinoptilolite-B_1 and Clinoptilolite-B_3 samples. In this case, it was stated by Elaiopoulos et al. (10) that as the pressure decreases, the separation of smaller pores may occur, and when the critical pressure value is lowered to a value, the separation of these micropores will be managed with a much slower progressing kinetics. It was stated that the equilibrium to be established between the adsorption and desorption phases would take longer time.

In this study, although there are differences in the surface morphology, area, total pore volume, and adsorption characteristics between the samples with the calcination process we applied, it is seen that the changes in the calcination temperature and time do not create very large differences between the pretreated samples. In their study, Elaiopoulos et al. (10) and Burris and Juenger (34) explained the calcination temperatures around 500-550 °C as moderate calcination temperatures and stated that the changes in the structure could be less at these calcination temperatures compared to higher temperatures. Burris and Juenger (34) stated that they observed a little decrease in the surface area and in the total pore volume depending on the calcination temperature values increasing from the calcination temperature of 300 °C. Although changes were observed after the calcinations performed at 300 and 500 °C, very large changes occurred after the calcination processes above 500 °C. Although it is stated that agglomeration can be seen in the structure as a result of sintering at temperatures, especially below 800 °C in their study, agglomeration did not occur at both calcination temperatures, as can be clearly seen in the SEM results of the author's study. Wang et al. (22) found that samples calcined at 800 °C had larger pore diameter and lower pore volume compared to samples calcined at 400 °C and 600 °C. Emphasizing that low calcination temperatures have negligible negative effects on the zeolite structure, they explained that increasing calcination temperatures damage the morphological structure. Elaiopoulos et al. (10) also determined that both agglomeration in the structure and a decrease in crystallinity can be observed due to the high temperature (above 550 °C) as a result of calcination. They stated that pores and channels may be clogged or damaged due to high-temperature-calcination. Depending on the increasing calcination temperatures, the calcination temperature of 300 and 500 °C was accepted to prevent both a decrease in the surface area and the agglomeration in the structure for this study. Unlike the Burris and Juenger (34) study, in this study, an increase in the surface area (except for Clinoptilolite-B_1 and Clinoptilolite-A_3 samples) and total pore volume was observed despite increasing calcination temperatures and time, thanks to the pre-treatment with acid before calcination. As mentioned before, pretreatment with acid provides these increases in surface area and total pore volume. Different researchers (22,25,35) also found a decrease in zeolite surface areas as a result of calcination. Florez et al. (35) emphasized that increasing calcination temperatures causes a reduction in total pore volume. Seraj et al. (25) stated that the decrease in the surface area is due to the destabilization of the zeolitic structure, the pores in the internal structure negatively affected, and the aggregation of the zeolite particles as a result of sintering. When this information is taken into account, the decrease in the surface area of the Clinoptilolite-A_3 and Clinoptilolite-B_1 samples in this study may have been caused by the instability of the zeolite structure or especially the pores in the internal structure negatively affected as a result of the calcination process. In other respects, as seen in Table 4, Clinoptilolite-B_2 and Clinoptilolite-B_3 samples show an increase in surface area compared to natural clinoptilolite sample (Clinoptilolite-B) with increasing calcination time and temperature despite the increasing pore diameter. This can be explained by the increase in the surface due to porosity in the material structure. Miądlicki et al. (43) reported that there may be an increase in porosity in acid-pretreated clinoptilolite samples. In addition, as seen in Clinoptilolite-B_3 SEM analysis, tabular, platy, and coffin-shaped structures in the samples may cause an increase in the surface area. According to Seraj et al. (25), since the BET surface area results take into account both the outer and inner surface area, it can also give an idea of the porosity of the material if the particle size distribution of the material is also known, as given in this study. When the samples with known BET surface area and particle size distribution are compared, the samples with larger pore diameters have a higher surface area, contrary to what it should be, which indicates that this material has more porosity.

Scanning Electron Microscopy (SEM) and Energy Dispersion Spectroscopy Analysis

The scanning electron microscopy images and EDS experiments were performed to examine the morphological properties and elemental composition belonging to the natural and treated clinoptilolites. SEM and EDS results for each sample are shown in Figures 11, 12, and 13 comparatively. Also, the average elemental compositions of

natural and treated clinoptilolites determined by EDS analysis are presented in Table 5.

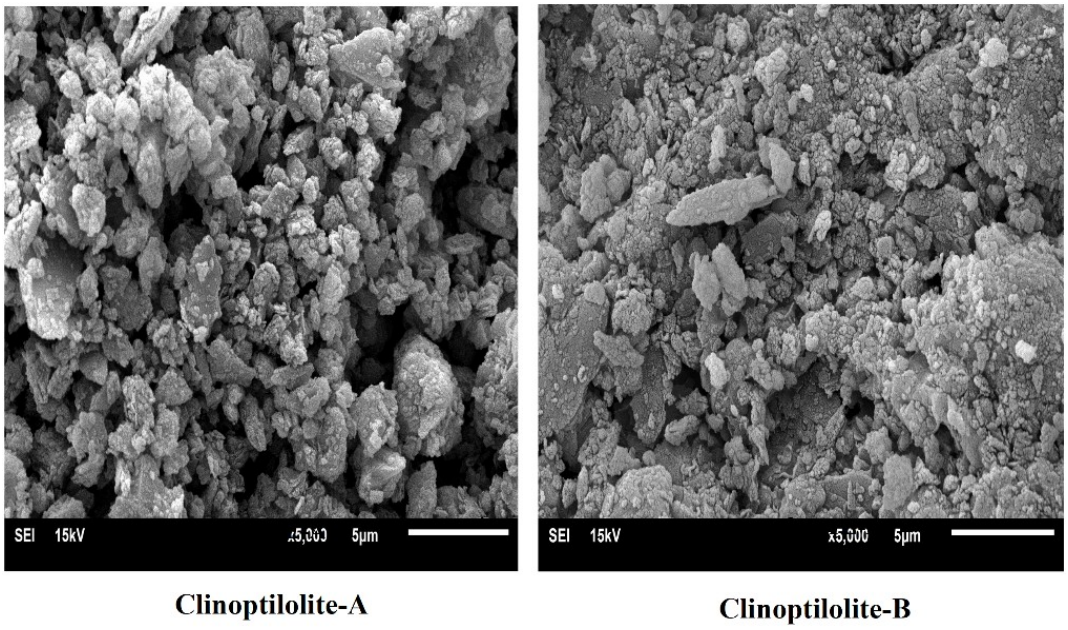

Figure 11: Morphological characterization determined with SEM for Clinoptilolite-A and Clinoptilolite-B.

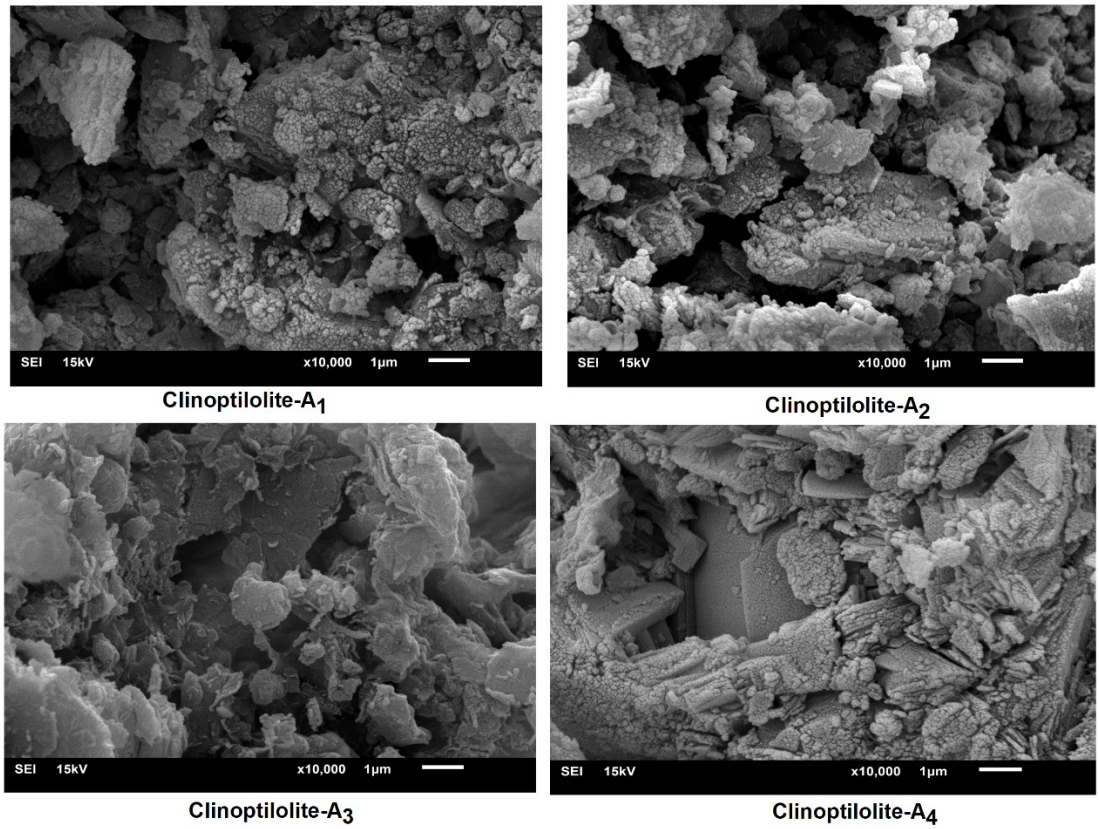

Figure 12: Morphological characterization determined with SEM for acid-treated clinoptilolites (modified from Clinoptilolite-A).

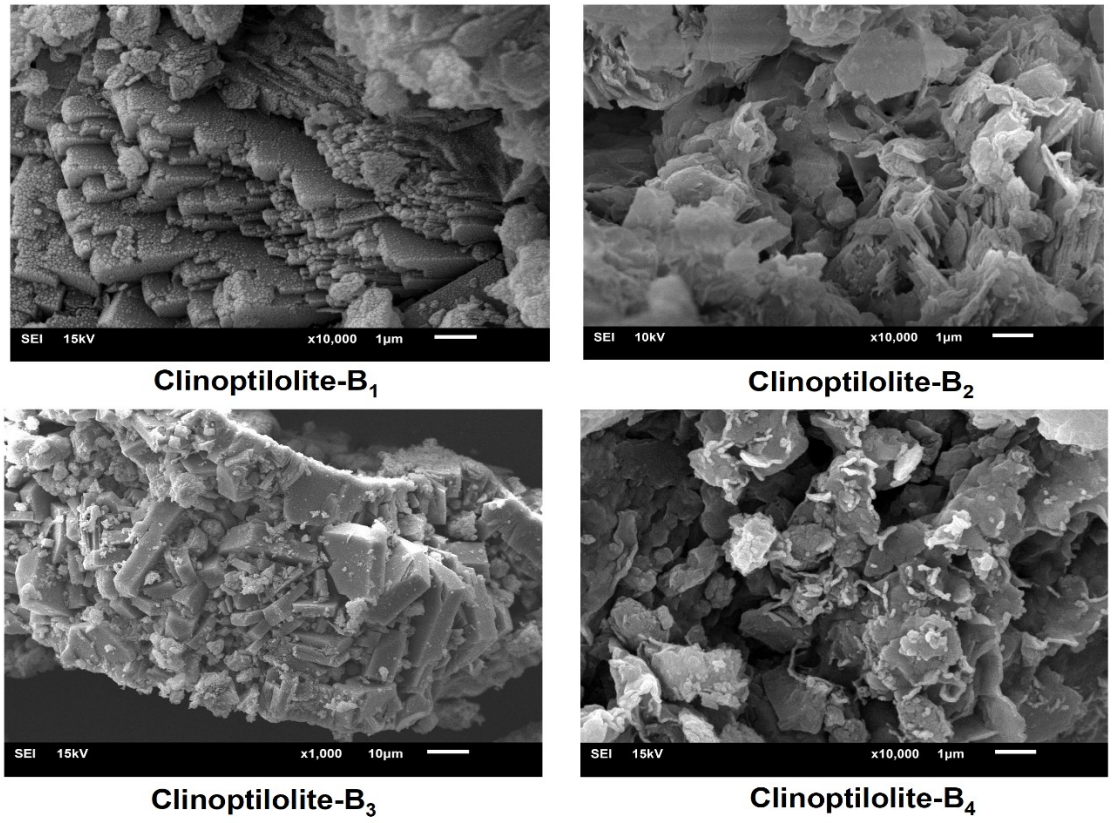

Figure 13: Morphological characterization determined with SEM for acid-treated clinoptilolites (modified from Clinoptilolite-B).

Table 5: Average elemental composition of natural and pre-treated clinoptilolites determined by EDS analysis.

Sample	O	Al	Si	Fe	Ca	K	C	Mg
Clinoptilolite-A	43.9	4.1	31.5	-	0.7	2.6	16.7	0.4
Clinoptilolite-A_1	40.3	4.9	30.6	1.7	0.9	1.5	19.6	0.5
Clinoptilolite-A_2	35.4	2.4	33.0	-	-	-	29.1	-
Clinoptilolite-A_3	46.1	4.5	23.4	0.9	0.4	1.5	22.8	0.4
Clinoptilolite-A_4	47.1	5.0	28.4	1.2	0.6	1.4	15.7	0.5
Clinoptilolite-B	41.5	5.5	27.4	2.0	1.6	2.8	18.7	0.4
Clinoptilolite-B_1	37.8	7.9	43.1	6.2	1.1	2.9	-	0.9
Clinoptilolite-B_2	42.3	5.0	27.2	1.8	0.7	2.0	20.5	0.4
Clinoptilolite-B_3	51.2	5.4	23.6	-	1.3	2.4	15.8	0.4
Clinoptilolite-B_4	44.6	5.4	25.5	2.0	0.7	1.5	19.7	0.6

.

Compared to natural zeolite samples; although there were differences in the morphological structure of the samples calcined at lower temperatures (300 °C) for both zeolite types, more significant changes were detected in the surface structure of the clinoptilolites calcined at higher temperatures (500 °C). In Figure 11, natural clinoptilolites are shown and, the particle structure of both is spherical and morphologically very similar to each other. After acid treatment and then calcination, except for the Clinoptilolite-A_1 sample, changes occurred in the structure with the increase in calcination temperature and time. When the calcination temperature was 500 °C, the particle structure began to transform from spherical to rod-shaped as seen in Figure 12. Compared to Clinoptilolite-A sample, although there were changes in the structure from the first calcination temperature for Clinoptilolite-B sample, significant changes occurred with the increase in calcination temperature and time. As in the other clinoptilolite sample, rod-shaped particles (especially Clinoptilolite-B_4) were detected more clearly when the calcination temperature was 500 °C in Figure 13. Additionally, tabular, platy, and coffin-shaped structures appeared in SEM images of Clinoptilolite-A_4, Clinoptilolite-B_1, and Clinoptilolite-B_3 as in several studies (10,38). It is seen that for both clinoptilolites, significant changes in the structure occur with the increase of the effect of calcination. Agudelo et al. (74) and Wang et al. (2) stated in their study that acid pretreatment did not cause significant changes in zeolite morphology. Also, Mortazavi et al. (12) carried out a different pretreatment using cations, amines, and ionic liquids and determined that there was no significant morphological difference between the pre-treated samples and natural clinoptilolites. In the study of Burris and Juenger (34), they detected agglomeration in the morphological structure of natural clinoptilolite after calcination at very high temperatures such as 965 °C. They determined that after all calcination processes at 300, 500, 800, and 965 °C, small particles were found on the larger zeolite structures in SEM images. In our study,

agglomeration was not observed after calcination, and the occurrence of smaller structures on large particles either did not occur or was negligible. Since the agglomeration seen in the structure is an important feature that restricts the use, and reduces the catalytic activity and selectivity, especially for catalytic purposes, it is very important to choose the most suitable pretreatment method for clinoptilolite and to determine the optimum conditions for this method. In addition, as we encountered in this study, the transformation of shapes of the particle into rod, platy or tabular structures as a result of the pre-treatment processes performed as an alternative to the spherical classical particle structure in the structure can provide advantages in different areas, especially for catalytic use.

The elemental compositions of the natural clinoptilolite and its treated versions were investigated with EDS carried out at 2 different random points. According to Table 5, the major elements of the natural clinoptilolite samples were O, Si, Al, and K additionally small amounts of Mg and Ca. It could be resulted from Table 5 that the amount of Ca and K decreased due to acid treatments and calcination. In the EDS analysis of the Clinoptilolite-B_1 a significant iron and aluminum content was determined compared to other samples. Only, Fe, Ca, K, and Mg content were not identified in Clinoptilolite-A_2. Mg content is similar to each other for all samples (except Clinoptilolite-A_2) correlated to XRF analysis results.

CONCLUSION

The effects of the pre-treatment procedure consisted of acid pretreatment and different calcination temperatures and durations on the main features of clinoptilolites were investigated by comparing with the characteristic features of the natural clinoptilolite sample. Treatment of clinoptilolite with HCl caused mild dealumination, removal of some cations, and impurities, resulting in an increase in surface area and total pore volume. Contrary to many studies in the literature, the suitability of calcination temperature and times in this study is an important result in that calcination does not adversely affect the surface properties of clinoptilolites. Treatment with HCl and calcination resulted in increased BET surface area and decreased mean pore diameter. As a result of pretreatment, there was a strong increase in N_2 adsorption isotherms, thanks to the removal of Al^{3+}, cations, possible amorphous structures, and impurities from the structure. The increased surface area values can be explained primarily by the presence of micropores. Depending on the increasing Si/Al ratios, an increase in BET surface areas was observed especially in Clinoptilolite-A_1, Clinoptilolite-A_2, Clinoptilolite-A_4, and Clinoptilolite-B_3 samples. In particular, the results of SEM and BET analysis support the conclusion that the pre-treatment method proposed in this study allows the preparation of non-agglomerated, non-sintered, large surface area clinoptilolites suitable for use as a catalyst, catalyst support, or adsorbent. The improvement of properties such as surface area and total pore volume were greater in the sample with smaller particle sizes. In addition, according to the results of thermogravimetric analysis, the weight loss of Clinoptilolite-B (except Clinoptilolite-B_2) with larger particle size and its pretreated modifications is higher than the pretreated Clinoptilolite-A samples. Although the untreated versions of both natural clinoptilolite samples gave chemically similar results, particle size differences resulted in differences in XRF results with applied pretreatments. These show that besides chemical or heat treatment, particle size and properties also determine the effect of these treatments on the structure. In future studies, we plan to apply for different uses of these pre-treated zeolites for catalyst, catalyst support, and hydrogen storage.

CONFLICT OF INTEREST

The author declares that she has no known competing financial interests or personal relationships that could have appeared to influence the work reported in this paper.

ACKNOWLEDGMENTS

This study was supported by the Yalova University Scientific Research Projects Unit through project No: 2019/AP/0014. I would like to express my sincere thanks to Gordes Zeolite Mining Corporation for their support in the supply of natural clinoptiolite samples. I also would like to thank Prof. Dr. Sibel BASAKCILARDAN KABAKCI for sharing her technical devices such as centrifuge and precision scales. I sincerely would like to thank Dr. Ozlem TUNA for her general support on the some technical issues.

REFERENCES

1. Çolak A, MİNdİVan F, Göktaş M. İndirgenmiş Grafen Oksit Katkılı UHMWPE Kompozitin Kuru ve Sulu Ortamlarda Aşınma Davranışlarının Karşılaştırılması. Nevşehir Bilim ve Teknoloji Dergisi. 2019 Dec 15;12–20. <DOI>.

2. Wang C, Leng S, Guo H, Cao L, Huang J. Acid and alkali treatments for regulation of hydrophilicity/hydrophobicity of natural zeolite. Applied Surface Science. 2019 Jun;478:319–26. <DOI>.

3. Ates A, Hardacre C. The effect of various treatment conditions on natural zeolites: Ion exchange, acidic, thermal and steam treatments. Journal of Colloid and Interface Science. 2012 Apr;372(1):130–40. <DOI>.

4. Silva M, Lecus A, Lin Y, Corrao J. Tailoring Natural Zeolites by Acid Treatments. MSCE. 2019;07(02):26–37. <DOI>.

5. Wang S, Peng Y. Natural zeolites as effective adsorbents in water and wastewater treatment. Chemical Engineering Journal. 2010 Jan 1;156(1):11–24. <DOI>.

6. Adinehvand J, Shokuhi Rad A, Tehrani AS. Acid-treated zeolite (clinoptilolite) and its potential to zinc removal from water sample. Int J Environ Sci Technol. 2016 Nov;13(11):2705–12. <DOI>.

7. Król MK, Jeleń P. The Effect of Heat Treatment on the Structure of Zeolite A. Materials. 2021 Aug 18;14(16):4642. <DOI>.

8. de Souza V, Villarroel-Rocha J, de Araújo M, Sapag K, Pergher S. Basic Treatment in Natural Clinoptilolite for Improvement of Physicochemical Properties. Minerals. 2018 Dec 14;8(12):595. <DOI>.

9. Cakicioglu-Ozkan F, Ulku S. The effect of HCl treatment on water vapor adsorption characteristics of clinoptilolite rich natural zeolite. Microporous and Mesoporous Materials. 2005 Jan;77(1):47–53. <DOI>.

10. Elaiopoulos K, Perraki Th, Grigoropoulou E. Monitoring the effect of hydrothermal treatments on the structure of a natural zeolite through a combined XRD, FTIR, XRF, SEM and N2-porosimetry analysis. Microporous and Mesoporous Materials. 2010 Oct;134(1–3):29–43. <DOI>.

11. Koshy N, Singh DN. Fly ash zeolites for water treatment applications. Journal of Environmental Chemical Engineering. 2016 Jun;4(2):1460–72. <DOI>.

12. Mortazavi N, Bahadori M, Marandi A, Tangestaninejad S, Moghadam M, Mirkhani V, et al. Enhancement of CO2 adsorption on natural zeolite, modified clinoptilolite with cations, amines and ionic liquids. Sustainable Chemistry and Pharmacy. 2021 Sep;22:100495. <DOI>.

13. Moshoeshoe M, Nadiye-Tabbiruka MS, Obuseng V. A review of the chemistry, structure, properties and applications of zeolites. Am J Mater Sci. 2017;7(5):196–221.

14. Dickerson T, Soria J. Catalytic Fast Pyrolysis: A Review. Energies. 2013 Jan 21;6(1):514–38. <DOI>.

15. Anand R, Khaire SS, Maheswari R, Gore KU. Alkylation of biphenyl with t-butylalcohol over modified Y zeolites. Journal of Molecular Catalysis A: Chemical. 2004 Aug;218(2):241–6. <DOI>.

16. Ivanova II, Kuznetsov AS, Yuschenko VV, Knyazeva EE. Design of composite micro/mesoporous molecular sieve catalysts. Pure and Applied Chemistry. 2004 Sep 30;76(9):1647–57. <DOI>.

17. Cherif L, El-Berrichi FZ, Benguedach A, Tougne P, Fraissard J. Structural evolution of calcium-exchanged (NH4)2SiF6-dealuminated Y zeolite after various chemical treatments. Colloids and Surfaces A: Physicochemical and Engineering Aspects. 2003 Jun;220(1–3):83–9. <DOI>.

18. Rivera A, Farías T, de Ménorval LC, Autié-Pérez M, Lam A. Natural and Sodium Clinoptilolites Submitted to Acid Treatments: Experimental and Theoretical Studies. J Phys Chem C. 2013 Feb 28;117(8):4079–88. <DOI>.

19. Valdiviés-Cruz K, Lam A, Zicovich-Wilson CM. Full Mechanism of Zeolite Dealumination in Aqueous Strong Acid Medium: Ab Initio Periodic Study on H-Clinoptilolite. J Phys Chem C. 2017 Feb 9;121(5):2652–60. <DOI>.

20. Panda AK, Mishra BG, Mishra DK, Singh RK. Effect of sulphuric acid treatment on the physico-chemical characteristics of kaolin clay. Colloids and Surfaces A: Physicochemical and Engineering Aspects. 2010 Jun;363(1–3):98–104. <DOI>.

21. Apelian MR, Fung AS, Kennedy GJ, Degnan TF. Dealumination of Zeolite β via Dicarboxylic Acid Treatment. J Phys Chem. 1996 Jan 1;100(41):16577–83. <DOI>.

22. Wang C, Cao L, Huang J. Influences of acid and heat treatments on the structure and water vapor adsorption property of natural zeolite. Surf Interface Anal. 2017 Dec;49(12):1249–55. <DOI>.

23. Chen X, Srubar WV. Sulfuric acid improves the reactivity of zeolites via dealumination. Construction and Building Materials. 2020 Dec;264:120648. <DOI>.

24. Ong LH, Dömök M, Olindo R, van Veen AC, Lercher JA. Dealumination of HZSM-5 via steam-treatment. Microporous and Mesoporous Materials. 2012 Dec;164:9–20. <DOI>.

25. Seraj S, Ferron RD, Juenger MCG. Calcining natural zeolites to improve their effect on cementitious mixture workability. Cement and Concrete Research. 2016 Jul;85:102–10. <DOI>.

26. Perraki T, Kontori E, Tsivilis S, Kakali G. The effect of zeolite on the properties and hydration of blended cements. Cement and Concrete Composites. 2010 Feb;32(2):128–33. <DOI>.

27. Li X, Qiao K, He L, Liu X, Yan Z, Xing W, et al. Combined modification of ultra-stable Y zeolites via citric acid and phosphoric acid. Appl Petrochem Res. 2014 Oct;4(4):343–9. <DOI>.

28. Matias P, Lopes JM, Ayrault P, Laforge S, Magnoux P, Guisnet M, et al. Effect of dealumination by acid treatment of a HMCM-22 zeolite on the acidity and activity of the pore systems. Applied Catalysis A: General. 2009 Aug;365(2):207–13. <DOI>.

29. Jentys A, Warecka G, Derewinski M, Lercher JA. Adsorption of water on ZSM 5 zeolites. J Phys Chem. 1989 Jun;93(12):4837–43. <DOI>.

30. Ahmadi B, Shekarchi M. Use of natural zeolite as a supplementary cementitious material. Cement and Concrete Composites. 2010 Feb;32(2):134–41. <DOI>.

31. Bilim C. Properties of cement mortars containing clinoptilolite as a supplementary cementitious material. Construction and Building Materials. 2011 Aug;25(8):3175–80. <DOI>.

32. Lilkov V, Petrov O, Petkova V, Petrova N, Tzvetanova Y. Study of the pozzolanic activity and hydration products of cement pastes with addition of natural zeolites. Clay miner. 2011 Jun;46(2):241–50. <DOI>.

33. Perraki T, Kontori E, Tsivilis S, Kakali G. The effect of zeolite on the properties and hydration of blended cements. Cement and Concrete Composites. 2010 Feb;32(2):128–33. <DOI>.

34. Burris LE, Juenger MCG. Effect of calcination on the reactivity of natural clinoptilolite zeolites used as supplementary cementitious materials. Construction and Building Materials. 2020 Oct;258:119988. <DOI>.

35. Florez C, Restrepo-Baena O, Tobon JI. Effects of calcination and milling pre-treatments on natural zeolites as a supplementary cementitious material. Construction and Building Materials. 2021 Dec;310:125220. <DOI>.

36. Roussel N, Lemaître A, Flatt RJ, Coussot P. Steady state flow of cement suspensions: A micromechanical state of the art. Cement and Concrete Research. 2010 Jan;40(1):77–84. <DOI>.

37. Fernandez R, Martirena F, Scrivener KL. The origin of the pozzolanic activity of calcined clay minerals: A comparison between kaolinite, illite and montmorillonite. Cement and Concrete Research. 2011 Jan;41(1):113–22. <DOI>.

38. Elaiopoulos K, Perraki Th, Grigoropoulou E. Mineralogical study and porosimetry measurements of zeolites from Scaloma area, Thrace, Greece. Microporous and Mesoporous Materials. 2008 Jul;112(1–3):441–9. <DOI>.

39. Erdoğan B, Dikmen G. Effect of the acid type on clinoptilolite-rich tuff for hydrogen storage. International Journal of Hydrogen Energy. 2020 Jan;45(3):2017–21. <DOI>.

40. Dziedzicka A, Sulikowski B, Ruggiero-Mikołajczyk M. Catalytic and physicochemical properties of modified natural clinoptilolite. Catalysis Today. 2016 Jan;259:50–8. <DOI>.

41. Davarpanah E, Armandi M, Hernández S, Fino D, Arletti R, Bensaid S, et al. CO2 capture on natural zeolite clinoptilolite: Effect of temperature and role of the adsorption sites. Journal of Environmental Management. 2020 Dec;275:111229. <DOI>.

42. Kennedy DA, Mujčin M, Abou-Zeid C, Tezel FH. Cation exchange modification of clinoptilolite –thermodynamic effects on adsorption separations of carbon dioxide, methane, and nitrogen. Microporous and Mesoporous Materials. 2019 Jan;274:327–41. <DOI>.

43. Miądlicki P, Wróblewska A, Kiełbasa K, Koren ZC, Michalkiewicz B. Sulfuric acid modified clinoptilolite as a solid green catalyst for solvent-free α-pinene isomerization process. Microporous and Mesoporous Materials. 2021 Sep;324:111266. <DOI>.

44. Ackley MW, Giese RF, Yang RT. Clinoptilolite: Untapped potential for kinetics gas separations. Zeolites. 1992 Sep;12(7):780–8. <DOI>.

45. Pabalan RT, Bertetti FP. Cation-Exchange Properties of Natural Zeolites. Reviews in Mineralogy and Geochemistry. 2001 Jan 1;45(1):453–518. <DOI>.

46. Moradi M, Karimzadeh R, Moosavi ES. Modified and ion exchanged clinoptilolite for the adsorptive removal of sulfur compounds in a model fuel: New adsorbents for desulfurization. Fuel. 2018 Apr;217:467–77. <DOI>.

47. Groen JC, Jansen JC, Moulijn JA, Perez-Ramirez J. Optimal Aluminum-Assisted Mesoporosity Development in MFI Zeolites by Desilication. ChemInform [Internet]. 2004 Nov 9 [cited 2022 Jun 13];35(45). <DOI>.

48. Erdoğan Alver B. A comparative adsorption study of C2H4 and SO2 on clinoptilolite-rich tuff: Effect of acid treatment. Journal of Hazardous Materials. 2013 Nov;262:627–33. <DOI>.

49. Nezamzadeh-Ejhieh A, Moazzeni N. Sunlight photodecolorization of a mixture of Methyl Orange and Bromocresol Green by CuS incorporated in a clinoptilolite zeolite as a heterogeneous catalyst. Journal of Industrial and Engineering Chemistry. 2013 Sep;19(5):1433–42. <DOI>.

50. Nezamzadeh-Ejhieh A, Amiri M. CuO supported Clinoptilolite towards solar photocatalytic degradation of p-aminophenol. Powder Technology. 2013 Feb;235:279–88. <DOI>.

51. Christidis G. Chemical and thermal modification of natural HEU-type zeolitic materials from Armenia, Georgia and Greece. Applied Clay Science. 2003 Nov;24(1–2):79–91. <DOI>.

52. Allen SJ, Ivanova E, Koumanova B. Adsorption of sulfur dioxide on chemically modified natural clinoptilolite. Acid modification. Chemical Engineering Journal. 2009 Oct 15;152(2–3):389–95. <DOI>.

53. Radosavljevic-Mihajlovic A, Dondur V, Dakovic A, Lemic J, Tomasevic-Canovic M. Physicochemical and structural characteristics of HEU-type zeolitic tuff treated by hydrochloric acid. J Serb Chem Soc. 2004;69(4):273–82. <DOI>.

54. Sakızcı M, Özgül Tanrıverdi L. Influence of acid and heavy metal cation exchange treatments on methane adsorption properties of mordenite. Turk J Chem. 2015;39:970–83. <DOI>.

55. Sato K, Nishimura Y, Matsubayashi N, Imamura M, Shimada H. Structural changes of Y zeolites during ion exchange treatment: effects of Si/Al ratio of the starting NaY. Microporous and Mesoporous Materials. 2003 May;59(2–3):133–46. <DOI>.

56. Korkuna O, Leboda R, Skubiszewska-Zie¸ba J, Vrublevs'ka T, Gun'ko VM, Ryczkowski J. Structural and physicochemical properties of natural zeolites: clinoptilolite and mordenite. Microporous and Mesoporous Materials. 2006 Jan;87(3):243–54. <DOI>.

57. Hyeon Kim M, Hwang UC, Nam IS, Gul Kim Y. The characteristics of a copper-exchanged natural zeolite for NO reduction by NH3 and C3H6. Catalysis Today. 1998 Sep;44(1–4):57–65. <DOI>.

58. Ruiz-Serrano D, Flores-Acosta M, Conde-Barajas E, Ramírez-Rosales D, Yáñez-Limón JM, Ramírez-Bon R. Study by XPS of different conditioning processes to improve the cation exchange in clinoptilolite. Journal of Molecular Structure. 2010 Sep;980(1–3):149–55. <DOI>.

59. Favvas EP, Tsanaktsidis CG, Sapalidis AA, Tzilantonis GT, Papageorgiou SK, Mitropoulos ACh. Clinoptilolite, a natural zeolite material: Structural characterization and performance evaluation on its dehydration properties of hydrocarbon-based fuels. Microporous and Mesoporous Materials. 2016 May;225:385–91. <DOI>.

60. Nezamzadeh-Ejhieh A, Shirzadi A. Enhancement of the photocatalytic activity of Ferrous Oxide by doping onto the nano-clinoptilolite particles towards photodegradation of tetracycline. Chemosphere. 2014 Jul;107:136–44. <DOI>.

61. Sánchez NA, Saniger JM, d'Espinose de la Caillerie JB, Blumenfeld AL, Fripiat JJ. Dealumination and surface fluorination of H-ZSM-5 by molecular fluorine. Microporous and Mesoporous Materials. 2001 Dec;50(1):41–52. <DOI>.

62. López-Fonseca R, de Rivas B, Gutiérrez-Ortiz JI, Aranzabal A, González-Velasco JR. Enhanced activity of zeolites by chemical dealumination for chlorinated VOC abatement. Applied Catalysis B: Environmental. 2003 Mar;41(1–2):31–42. <DOI>.

63. Blancovarela M, Martinezramirez S, Erena I, Gener M, Carmona P. Characterization and pozzolanicity of zeolitic rocks from two Cuban deposits. Applied Clay Science. 2006 Jul;33(2):149–59. <DOI>.

64. Aghadavoud A, Rezaee Ebrahim Saraee K, Shakur HR, Sayyari R. Removal of uranium ions from synthetic wastewater using ZnO/Na-clinoptilolite nanocomposites. Radiochimica Acta. 2016 Nov 1;104(11):809–19. <DOI>.

65. Mozgawa W. The relation between structure and vibrational spectra of natural zeolites. Journal of Molecular Structure. 2001 Sep;596(1–3):129–37. <DOI>.

66. Ramishvili T, Tsitsishvili V, Chedia R, Sanaia E, Gabunia V, Kokiashvili N. Preparation of ultradispersed crystallites of modified natural clinoptilolite with the use of ultrasound and its application as a catalyst in the synthesis of methyl salicylate. American Journal of Nano Research and Applications. 2017;5(3–1):26–32.

67. Mozgawa W, Fojud Z, Handke M, Jurga S. MAS NMR and FTIR spectra of framework aluminosilicates. Journal of Molecular Structure. 2002 Sep;614(1–3):281–7. <DOI>.

68. Lutz W, Rüscher CH, Heidemann D. Determination of the framework and non-framework [SiO2] and [AlO2] species of steamed and leached faujasite type zeolites: calibration of IR, NMR, and XRD data by chemical methods. Microporous and Mesoporous Materials. 2002 Sep;55(2):193–202. <DOI>.

69. Perraki Th, Orfanoudaki A. Mineralogical study of zeolites from Pentalofos area, Thrace, Greece. Applied Clay Science. 2004 Apr;25(1–2):9–16. <DOI>.

70. Akbelen M, Ezber Ç. Investigation of thermal and structural properties of nitric, hydrochloric and sulphuric acid-treated zeolite. Eskişehir Technical University Journal of Science and Technology A - Applied Sciences and Engineering [Internet]. 2019 Dec 16 [cited 2022 Jun 13]; <DOI>.

71. Kowalczyk P, Sprynskyy M, Terzyk AP, Lebedynets M, Namieśnik J, Buszewski B. Porous structure of natural and modified clinoptilolites. Journal of Colloid and Interface Science. 2006 May;297(1):77–85. <DOI>.

72. Elizalde-González MP, Mattusch J, Wennrich R, Morgenstern P. Uptake of arsenite and arsenate by clinoptilolite-rich tuffs. Microporous and Mesoporous Materials. 2001 Aug;46(2–3):277–86. <DOI>.

73. Segawa K, Shimura T. Effect of dealumination of mordenite by acid leaching for selective synthesis of ethylenediamine from ethanolamine. Applied Catalysis A: General. 2000 Mar;194–195:309–17. <DOI>.

74. Agudelo JL, Hensen EJM, Giraldo SA, Hoyos LJ. Influence of steam-calcination and acid leaching treatment on the VGO hydrocracking performance of faujasite zeolite. Fuel Processing Technology. 2015 May;133:89–96. <DOI>.